Supplementary Material: Reversal mechanism of an individual Ni nanotube simultaneously studied by torque and SQUID magnetometry

A. Buchter[1], J. Nagel[2], D. Rüffer[3], F. Xue[1], D. P. Weber[1], O. F. Kieler[4], T. Weimann[4], J. Kohlmann[4], A. B. Zorin[4], E. Russo-Averchi[3], R. Huber[5], P. Berberich[5], J. Arbiol[6], A. Fontcuberta i Morral[3], M. Kemmler[2], R. Kleiner[2], D. Koelle[2], D. Grundler[5,7]* and M. Poggio[1]†

[1]*Department of Physics, University of Basel, 4056 Basel, Switzerland;*

[2]*Physikalisches Institut and Center for Collective Quantum Phenomena in LISA+,*
Universität Tübingen, 72076 Tübingen, Germany;

[3]*Laboratoire des Matériaux Semiconducteurs, Institut des Matériaux,*
Ecole Polytechnique Fédérale de Lausanne, 1015 Lausanne, Switzerland;

[4]*Fachbereich 2.4 "Quantenelektronik",*
Physikalisch-Technische Bundesanstalt, 38116 Braunschweig, Germany;

[5]*Lehrstuhl für Physik funktionaler Schichtsysteme, Physik Department E10,*
Technische Universität München, 85747 Garching, Germany;

[6]*Institució Catalana de Recerca i Estudis Avançats and Institut de*
Ciència de Materials de Barcelona, 08193 Bellaterra, CAT, Spain

[7]*Faculté Sciences et Technique de l'Ingénieur,*
Ecole Polytechnique Fédérale de Lausanne, 1015 Lausanne, Switzerland

EXPERIMENTAL METHODS

NanoSQUID Device

The small loop-size of the nanometer-scale superconducting quantum interference device (nanoSQUID), as shown in Fig. S 1, encloses an area $\approx 0.4\,\mu\mathrm{m}^2$, resulting in an inductance of about $2\,\mathrm{pH}$. In a shielded environment [1], the nanoSQUID used here has a rms flux noise $S_\Phi^{1/2} = 200\,\mathrm{n}\Phi_0/\sqrt{\mathrm{Hz}}$ above $\sim 1\,\mathrm{kHz}$, where $\Phi_0 = \frac{h}{2e}$, h is Planck's constant, and e is the fundamental charge. An on-chip modulation line in the bottom Nb layer along $\hat{x}$ is used to couple a magnetic flux $\Phi_{\mathrm{mod}} \propto I_{\mathrm{mod}}$ to the SQUID, where I_{mod} is the modulation current. A flux-locked-loop (FLL) locks the nanoSQUID to its optimal working point and linearizes its output voltage $V_{\mathrm{out}}/\Phi = 2.55\,\mathrm{V}/\Phi_0$.
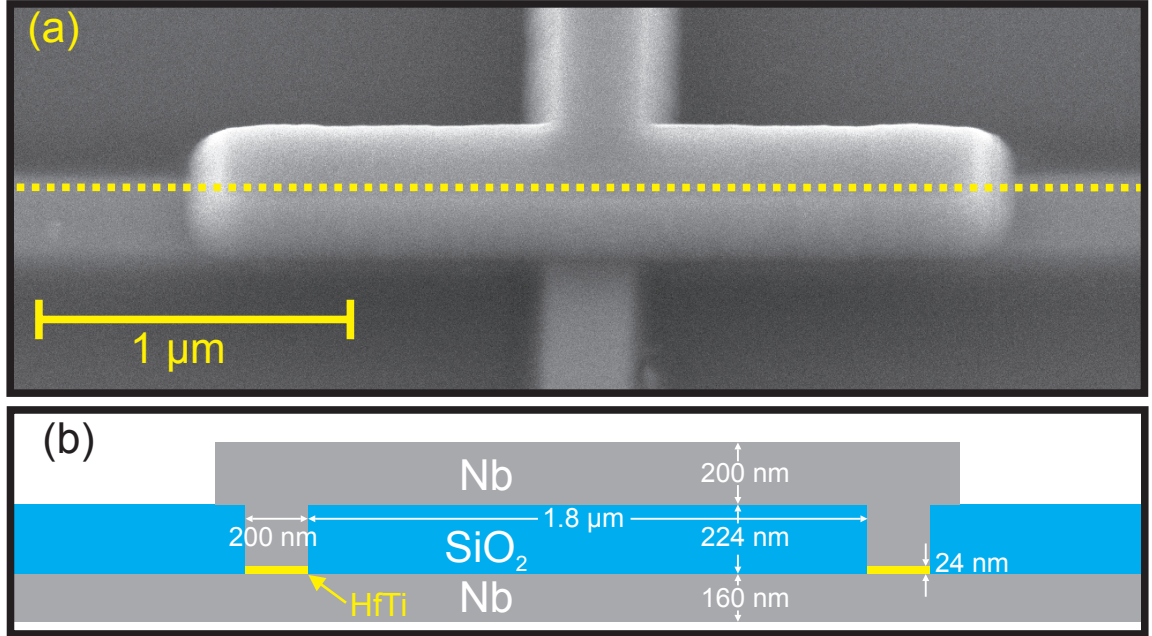

Fig. S 1: The nanoSQUID device. (a) A scanning electron micrograph (SEM) of the device and (b) a cross-sectional diagram of its structure in the plane of constant y defined by the dotted line in (a).

Cantilever Frequency Measurement

The 10-μm-wide paddle near the cantilever tip is used as one reflector of the optical fiber interferometer; the other is the cleaved end of an optical fiber, on which a thin layer of Si has been evaporated in order to match the cantilever reflectivity. 100 nW of laser light at a wavelength of 1550 nm are used in the interferometer in order to detect deflections of the cantilever along $\hat{y}$. The interferometric signal is fed through a field programmable gate array circuit back to a piezoelectric element which is mechanically coupled to the cantilever. This feedback is used to self-oscillate the cantilever at a given amplitude (typically 50 nm$_{\mathrm{rms}}$), enabling fast and accurate measurement of its fundamental resonance frequency f_c.

Experimental Protocol

To ensure that the experiments – especially scans of $\Phi(x, y)$ and $\Delta f(x, y)$ – start with the nanotube in a well-defined magnetic state, we first saturate it along its easy axis ($\hat{z}$) by applying $\mu_0 H = 150$ mT. To avoid trapped flux in the nanoSQUID, this saturation is performed at $T = 14$ K, above its transition temperature $T_c = 9$ K. Then, before scanning, which is performed at $\mu_0 H = 0$, the nanoSQUID is zero-field cooled to $T = 4.3$ K and locked to its working point using the FLL.

Ni Nanotube Fabrication

The Ni nanotubes are fabricated by atomic layer deposition (ALD). The reaction chamber and the ALD substrate holder containing the GaAs nanotemplate are heated to $300\,°C$. As a first step, a 20-nm-thick layer of Al_2O_3 is deposited using trimethylaluminium and water with standard ALD process parameters. Second, for the deposition of Ni, the precursor material $NiCp_2$ is heated to a temperature of about $130\,°C$ to provide the relevant vapor pressure in the source container. The ALD process flow for Ni consists of a sequence of injection and purging pulses using inert Ar gas, which is repeated 800 times to form a Ni layer of 40 nm. The sequentially injected materials and gases are $NiCp_2$, ozone, and hydrogen, each followed by a purging process to remove residuals from the gas atmosphere of the ALD reaction chamber. The process reads as follows:

$$800 \times (0.8 \text{ s}|4 \text{ s} + 10 \text{ s}|10.0 \text{ s} + 16 \text{ s}|20 \text{ s}), \tag{1}$$

Here, the first two numbers give the durations of the injection and purge pulses of precursor $NiCp_2$ and Ar, respectively. The third and fourth numbers provide the injection and purge time of O_3 and Ar, respectively; the fifth and sixth numbers define the hydrogen injection and Ar purge time, respectively. Long purging times are used to avoid an explosive mixture of H_2 and O_3 in the pumping line. On a flat substrate, smooth thin films are obtained. On curved nanotemplates, such as the GaAs template nanowires, the shell material shows more roughness than observed in flat films. The smoothness of these shells may be improved by both increasing the injection times of $NiCp_2$ and decreasing the substrate temperature. We expect the surface of the Ni to oxidize in ambient atmosphere.

Measurement of Ni Nanotube Volume

In Fig. S 2, we show a transmission electron micrograph (TEM) and a SEM of a Ni nanotube similar to that measured in our measurements. Grown in the same batch and on the same wafer, this nanotube should have identical properties as the measured tube within the natural variation of the growth process. Note the surface roughness, which is responsible for the error in the determination of the Ni nanotube's outer diameter. An average outer and inner diameter is determined by measuring many nanotubes in TEMs and SEMs such as these. The length of the Ni nanotube is determined with an optical microscope. Its volume V_{Ni} is then calculated from these parameters with the uncertainty in outer diameter contributing the largest error. This error is eventually responsible for most of the uncertainty in the saturation magnetization M_{S} and anisotropy parameters K, which we extract for the Ni nanotube.
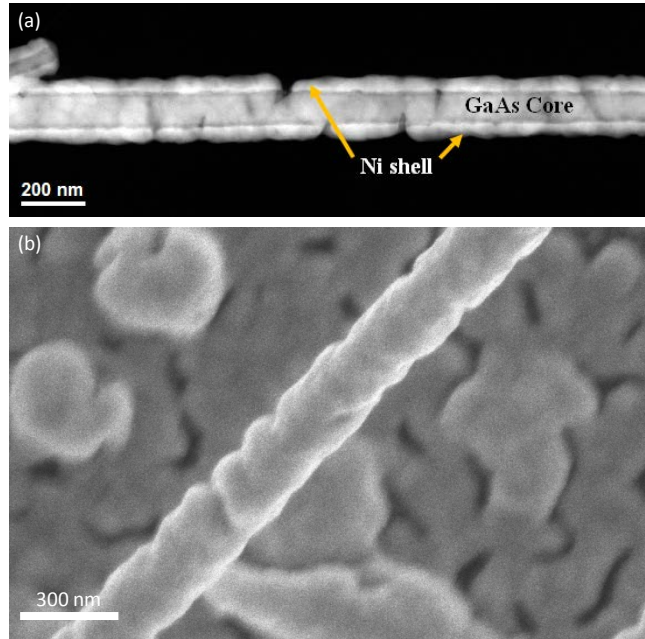

Fig. S 2: (a) TEM and (b) SEM of Ni nanotubes grown in the same batch and on the same wafer as that measured in the experiments.

FURTHER FLUX HYSTERESIS LOOPS

We record further hysteresis loops of $\Phi_{NN}(H)$ under similar conditions to that shown in Fig. 2 of the main text and plot them in Fig. S 3. The switching fields $H_{sw,e}$ are seen to vary from sweep to sweep. Nevertheless, as in the main text, they are observed to occur for $15 \text{ mT} < \mu_0|H_{sw,e}| < 35 \text{ mT}$. The consistently asymmetric behavior at positive and negative fields may be due to an anti-ferromagnetic NiO surface layer providing exchange interaction with the Ni nanotube [2, 3].
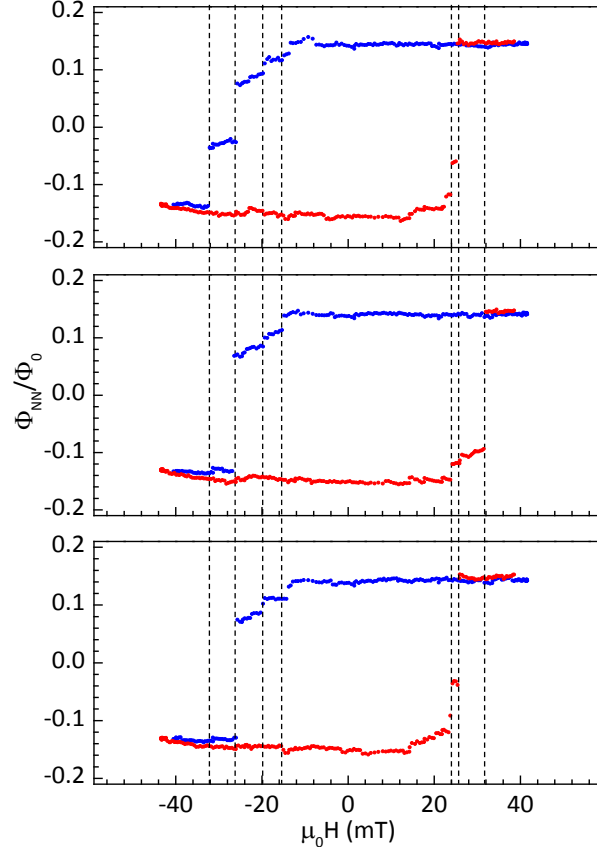

Fig. S 3: Hysteresis loops of $\Phi_{NN}(H)$ at $z = 280$ nm. Red (blue) points represent data taken while sweeping H in the positive (negative) direction. Dashed lines indicate magnetic switching fields $H_{sw,e}$.

SIMULATED VOLUME MAGNETIZATION AND LOCAL STRAY FLUX

In addition to simulating the volume magnetization $M(H)$ of the Ni nanotubes, we also use the NMAG package [4] to calculate the stray field at the position of the nanoSQUID. The results allow us to determine the predicted stray flux $\Phi_{NN}(H)$ coupling to the nanoSQUID for each simulated nanotube. The shapes of the simulated $\Phi_{NN}(H)$ are at all positions and for all nanotube lengths l nearly proportional to $M(H)$ and thus closely follow the shape of the corresponding $M(H)$. An example of a simulated hysteresis loop is plotted together with the measured $M(H)$ in Fig. S 4. Considering a segment of $l = 500$ nml the large jump observed in $M(H)$ near ± 30 mT is reproduced. We expect the further jumps to occur from other segments with slightly longer or shorter l, which contribute to the measured magnetization of the tube.
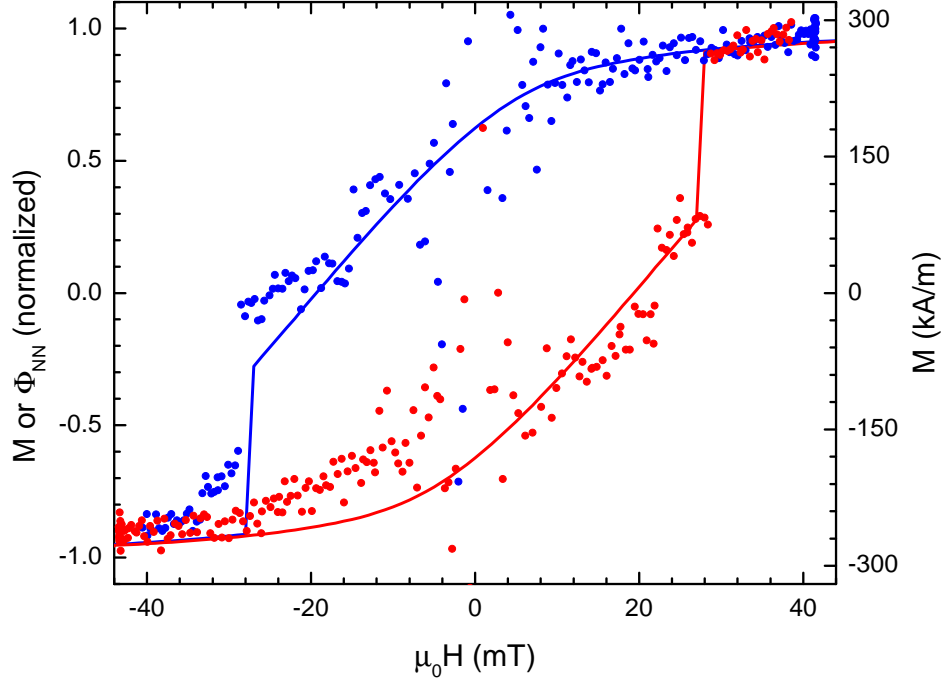
Fig. S 4: Hysteresis loops of $M(H)$ or $\Phi_{\mathrm{NN}}(H)$ simulated by NMAG (lines) and $M(H)$ measured by cantilever magnetometry (points). The Ni nanotube is simulated with $l = 500$ nm and $\Phi_{\mathrm{NN}}(H)$ is calculated with the tube positioned as in the experiments, i.e. at a position of optimal coupling for $z = 450$ nm. The measured data is the same as plotted in Fig. 3 (c). Red (blue) represent sweeps of H in the positive (negative) direction. The left (right) axis corresponds to the simulated (measured) data.

SIMULTANEOUS DETECTION OF SWITCHING EVENTS

We further investigate the switching of magnetic domains by sweeping H through the coercive field with the Ni nanotube optimally positioned at $z = 200\,\text{nm}$. During the sweep, we measure the cantilever displacement y and the flux Φ coupled into the nanoSQUID. To achieve maximum bandwidth the SQUID is operated in open-loop-mode for these experiments, such that a flux Φ produces a response voltage $V_{\text{OL}} \approx V_0 \sin(\Phi/\Phi_0 + \theta) + V_{\text{offset}}$, where $V_0 = 20\,\mu\text{V}$ in our experiment, θ is a phase factor, and V_{offset} is determined by choice of the SQUID's working-point. A peak-to-peak noise amplitude of $4\,\mu\text{V}$ is the result of the room-temperature amplifier used. Fig. S 5 (a) shows y and V_{OL} recorded while $\mu_0 H$ is swept at $1.5\,\text{mT/s}$ in a field range where magnetization switching is not expected. V_{OL} undergoes a roughly sinusoidal oscillation of less than one full period, consistent with the change in flux expected from sweeping H. Fluctuations in y with an amplitude of around 5 nm are attributed to the cantilever's thermal noise at $4.3\,\text{K}$.
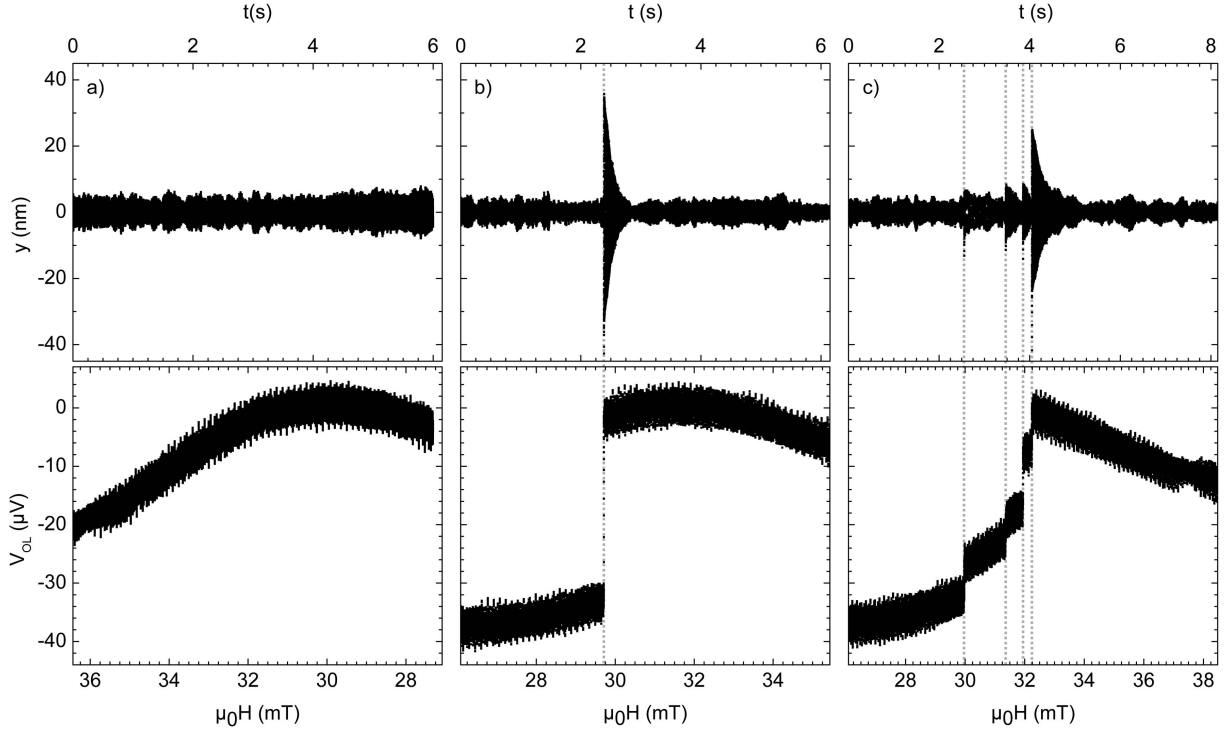

Fig. S 5: Simultaneous measurements of $y(t)$ and $\Phi(t)$ at $z = 200\,\mu\text{m}$ and an xy-position of optimal coupling. Representative data acquired while sweeping H (a) far from the coercive field and (b), (c) across the coercive field.

In Figs. S 5 (b) and (c), y and V_{OL} are recorded while the field is swept at $1.5\,\mathrm{mT/s}$ in a field range where switching is expected. In the first $2.3\,\mathrm{s}$ of the sweep shown in (b), the cantilever displacement is given by thermal noise and and the flux coupled to the nanoSQUID is free of discontinuities. As a field of $29.7\,\mathrm{mT}$ is reached, the cantilever displacement shows a sharp increase in amplitude from $5\,\mathrm{nm}$ to $35\,\mathrm{nm}$ followed by an a exponential decay back to the thermal noise level at around $5\,\mathrm{nm}$. The rise-time is limited by the cantilever's oscillation period. Simultaneous to this mechanical excitation, we observe a jump in V_{OL}. The rising edge is limited by the bandwidth of the preamplifier. Another instance of this behavior is presented in Fig. S 5 (c) where the field is again swept through the nanotube's coercive field. Between 30 and $32\,\mathrm{mT}$, a series of four excitations with varying amplitude appear both in the cantilever displacement and in the nanoSQUID flux. These two examples are representative of a number of traces taken under the same conditions. The decay time of the mechanical excitations for all events is $\tau \simeq 200$ ms, corresponding to a quality factor $Q = \pi f_0 \tau \simeq 2 \times 10^3$. This quality factor is one order of magnitude smaller than Q_0. We attribute the reduction to dissipative interactions between the Ni nanotube-tipped cantilever and the nanoSQUID device.

These sudden excitations, given their signature in both the cantilever displacement and the nanoSQUID flux, represent the switching of magnetization domains within the Ni nanotube. On the one hand, the reorientation of a magnetic domain exerts a torque on the cantilever in the presence of an external field and causes its mechanical excitation. On the other hand, the same reorientation suddenly alters the stray field coupled from the Ni nanotube to the nanoSQUID. The kinetic energy imparted to the cantilever by the switching event is estimated as $E_{\mathrm{kin}} = \frac{k}{2\Delta t} \int_t^{t+\Delta t} (y^2 - y_{th}^2) \mathrm{d}t$, where t is the time of the excitation, Δt is its duration, and y_{th} is the rms thermal displacement. The magnetic potential energy released in a complete magnetization reversal at field $H_{\mathrm{sw,e}}$ is given by $E_{mag} = M_s V_{\mathrm{Ni}} \mu_0 H_{\mathrm{sw,e}}$, where M_s is the saturation magnetization of the Ni nanotube and V_{Ni} its volume. For the switching events shown in Figs. S 5 (b) and (c), the magnetic potential energy is estimated to be $E_{mag} \simeq 3.9 \times 10^{-16}$ J, exceeding the corresponding E_{kin} of the excitations by four orders of magnitude. The large majority of the magnetic potential energy is therefore not captured as oscillations of the cantilever's fundamental mode, possibly dissipating into higher order mechanical modes, as phonons, or as electromagnetic radiation.

* Electronic address: grundler@ph.tum.de

† Electronic address: martino.poggio@unibas.ch

[1] R. Wölbing, J. Nagel, T. Schwarz, O. Kieler, T. Weimann, J. Kohlmann, A. Zorin, M. Kemmler, R. Kleiner, and D. Koelle, *Appl. Phys. Lett.* **102**, 192601 (2013).

[2] P. Zhang, F. Zuo, F. K. Urban III, A Khabari, P. Griffiths, and A. Hosseini-Tehrani, *J. Magn. Magn. Mater.* **225**, 337 (2000).

[3] M. Gierlings, M. J. Prandolini, H. Fritzsche, M. Gruyters, and D. Riegel, *Phys. Rev. B* **65**, 092407 (2002).

[4] T. Fischbacher, M. Franchin, G. Bordignon, H. Fangohr, *IEEE Trans. Magn.* **43**, 2896 (2007); http://nmag.soton.ac.uk/nmag/.